Research Square

Preprints are preliminary reports that have not undergone peer review.
They should not be considered conclusive, used to inform clinical practice,
or referenced by the media as validated information.

Enhancement of Bipartite Entanglement in Three Level Lasers via Kerr Resonator Coupled to Squeezed Vacuum Reservoir

Sisay Belachew

sisaybelachew@obu.edu.et

Oda Bultum University

Firomsa Feyissa

Oda Bultum University

Mohammed Kelif

Oda Bultum University

Research Article

Keywords: continuous variable, Kerr nonlinearity, spontaneous emission

Posted Date: September 7th, 2026

DOI: https://doi.org/10.21203/rs.3.rs-10802281/v1

License: This work is licensed under a Creative Commons Attribution 4.0 International License.
Read Full License

Additional Declarations: No competing interests reported.

Enhancement of Bipartite Entanglement in Three Level Lasers via Kerr Resonator Coupled to Squeezed Vacuum Reservoir

Sisay Belachew[1*], Firomsa Feyissa[2] and Mohammed Kelif[3]

[1,2,3]Department of Physics, Oda Bultum University, Chiro, 226, Oromia, Ethiopia.

*Corresponding author(s). E-mail(s): sbelachew9@gmail.com;
Contributing authors: firomsafeyissa@obu.edu.et;
momahedkelifa@obu.edu.et;

Abstract

On this paper, We investigate the generation and enhancement of bipartite entanglement in a three level cascade laser embedded in a Kerr nonlinear resonator and coupled to a squeezed vacuum reservoir. The system dynamics are modeled using a quantum master equation that incorporates atom-field interactions, Kerr nonlinearity, cavity damping, spontaneous emission, and squeezed vacuum effects. Applying the good cavity approximation, the atomic variables are adiabatically eliminated to derive effective cavity-field equations, which are transformed into c-number Langevin equations. Linearization around the steady state yields analytical expressions for second-order moments and the covariance matrix. Bipartite entanglement is quantified using the Duan inseparability criterion and logarithmic negativity. Our numerical results show that stronger Kerr nonlinearity and more squeezing greatly increase quantum correlations, while coherent pumping improves entanglement by boosting atomic coherence.However, higher cavity losses reduce entanglement due to photon loss.These findings highlight Kerr-enhanced cascade lasers with squeezed reservoirs as potential sources of entangled light for engineering bright, highly entangled CV optical sources for quantum key distribution, teleportation, and optical quantum networks.

Keywords: continuous variable, Kerr nonlinearity, spontaneous emission

1 Introduction

Quantum entanglement is a fundamental concept in modern quantum physics and is essential for creating nonclassical connections used in quantum communication, teleportation, and computing. It allows for strong correlations between quantum systems that are separated in space, which cannot be explained by classical physics.Continuous variable (CV) entanglement, which is made using the amplitude properties of light waves, has become very popular because it is strong, can be made reliably, and works well with existing technologies for sending light signals [1, 2]. As a result, CV entangled states are now vital for many quantum applications like teleportation, secure communication, data compression, networked quantum systems, sensing, and information processing [3–8].

Optical systems, especially those involving lasers and materials that change their properties in response to light, are practical ways to create entangled light. Three level laser systems are particularly interesting because they have simple structures and allow for strong interactions between atoms and light. Adding nonlinear optical materials, such as Kerr media, can change the behavior of light significantly [9–11]. These materials alter the refractive index based on light intensity, which leads to interactions between photons inside an optical cavity. These nonlinear effects can increase quantum correlations and help create entangled states. Another method to improve quantum correlations is by connecting the system to a squeezed vacuum. A squeezed vacuum is a special kind of light where the random fluctuations in one property are lower than usual, which can lead to stronger connections between different parts of the light and improve entanglement.

Among the different systems used to generate entangled light, three-level cascade lasers are getting a lot of attention because they naturally produce pairs of correlated photons through a process involving atomic transitions [12, 13]. The interaction between the laser cavity and the atoms creates coherence, which is key in forming quantum connections between different parts of the light[14–16]. The optical Kerr effect causes changes in the light's path based on its own intensity, resulting in interactions between photons. These interactions change the behavior inside the cavity, and can lead to stronger squeezing and entanglement by making the cavity's parts interact more effectively. Unlike a regular vacuum, which only adds typical noise from random fluctuations, a squeezed vacuum has strong connections between pairs of photons [17]. This reduces noise in one part of the light while increasing it in another. Putting squeezed vacuum into an optical cavity can greatly boost the squeezing effect, reduce loss of quantum properties, and improve entanglement by transferring correlations from the reservoir to the light inside the cavity. Even though each of these methods Kerr nonlinearity, squeezed vacuum, and three level lasers has been studied a lot on its own, they are usually looked at separately. Few studies have explored how these effects work together in a single model. Since these effects come from different physical processes, using them together might create even stronger quantum correlations than using just one [18]. Therefore, a thorough theoretical study is needed to understand how these effects can work together to improve entanglement.

In this study, we carry out a comprehensive quantum analysis of a three level cascade laser system that is placed inside a Kerr nonlinear cavity and coupled to

a squeezed vacuum reservoir. Previous studies have shown that Kerr nonlinearity enhances quantum correlations through self phase and cross phase modulation, while squeezed vacuum reservoirs reduce quantum noise and improve continuous variable entanglement and three level cascade lasers have been widely studied as efficient sources of correlated photon pairs. However, a comprehensive theoretical framework that simultaneously incorporates Kerr nonlinear coefficient, squeezing parameter, coherent pump strength, and cavity decay rate has not been systematically investigated within a unified master equation and Heisenberg Langevin equation. To address this gap, the present work develops a comprehensive theoretical model of a three-level cascade laser embedded in a Kerr resonator and coupled to a squeezed vacuum reservoir. Starting from the Hamiltonian system and the Lindblad master equation to obtain the corresponding Heisenberg Langevin equations with eliminate the atomic variables under the good cavity approximation and derive analytical expressions for the second order moments we quantified continuous variable entanglement using both the Duan inseparability criterion and logarithmic negativity.

2 Model and Hamiltonian Formulation

Our system of model analysis that the cooperative interplay between Kerr nonlinear coefficient, squeezing parameter and coherent pump strength correlations in a three level cascade laser are powerful quantum resources for enhancing squeezing and continuous variable entanglement for engineering highly entangled optical fields for continuous variable quantum communication and quantum information processing as see from figure 1. The interaction of the system can be described using the Hamilto-

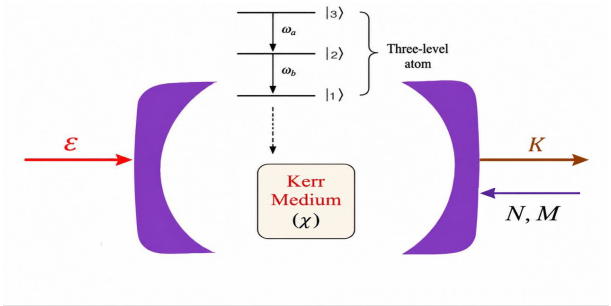


Figure 1

nian consider a cascade three-level laser consisting of atoms with energy levels $|3\rangle$, $|2\rangle$, and $|1\rangle$ interacting with two cavity modes a and b. The cavity contains a Kerr nonlinear medium and is coupled to a broadband squeezed vacuum reservoir. The total Hamiltonian of the system can be written as

$$\hat{H} = \hat{H}_0 + \hat{H}_{AF} + \hat{H}_P + \hat{H}_K, \tag{1}$$

where $\hat{H}_0$ is the free Hamiltonian,

$$\hat{H}_0 = \sum_{i=1}^{3} \hbar\omega_i |i\rangle\langle i| + \hbar\omega_a \hat{a}^\dagger \hat{a} + \hbar\omega_b \hat{b}^\dagger \hat{b}, \tag{2}$$

where ω_i denotes the energy of the atomic level $|i\rangle$, a ($a^\dagger$) and b ($b^\dagger$) are the annihilation (creation) operators corresponding to the two cavity modes, while ω_a and ω_b are the frequencies of the cavity modes associated with the transitions $|3\rangle \longrightarrow |2\rangle$ and $|2\rangle \longrightarrow |1\rangle$, respectively. The operators $\hat{a}^\dagger$ and $\hat{a}$ ($\hat{b}^\dagger$ and $\hat{b}$) satisfy the bosonic commutation relations

$$[\hat{a}, \hat{a}^\dagger] = 1, \quad [\hat{b}, \hat{b}^\dagger] = 1.$$

Eq. (2) represents the free Hamiltonian of the uncoupled atom cavity system. The first term describes the energy of the three atomic levels, while the second and third terms correspond to the free energies of cavity modes a and b. This Hamiltonian serves as the reference for transforming the system into the interaction picture. Under the electric dipole and rotating wave approximations, the interaction between the three-level atom and the cavity modes is described by

$$\hat{H}_{AF} = \hbar g_a \left(\hat{a}\hat{\sigma}_{32} + \hat{a}^\dagger \hat{\sigma}_{23}\right) + \hbar g_b \left(\hat{b}\hat{\sigma}_{21} + \hat{b}^\dagger \hat{\sigma}_{12}\right), \tag{3}$$

where $\hat{\sigma}_{ij} = |i\rangle\langle j|$ and g_a and g_b are the atom-cavity coupling constants. The coupling constants are characterize the strength of the interaction between the atoms and the respective cavity modes.

To induce coherence between the upper and lower atomic states, an external classical coherent field drives the dipole-forbidden transition $|3\rangle \longrightarrow |1\rangle$. The corresponding Hamiltonian is

$$\hat{H}_P = \frac{\hbar\Omega_p}{2} \left(e^{-i\omega_p t}\hat{\sigma}_{31} + e^{i\omega_p t}\hat{\sigma}_{13}\right), \tag{4}$$

where Ω_p is the Rabi frequency of the driving field and ω_p denotes its angular frequency [19]. Under exact resonance, the time-dependent phase factors disappear in the interaction picture [20], giving

$$\hat{H}_P = \frac{\hbar\Omega_p}{2} \left(\hat{\sigma}_{31} + \hat{\sigma}_{13}\right). \tag{5}$$

Eq.5 show the coherent pump prepares atomic coherence that is transferred to the cavity field, increasing the degree of quantum correlation between the emitted photons. As a result, the cavity resonance frequency becomes intensity dependent, giving rise to nonlinear optical phenomena such as self-phase modulation, cross-phase modulation, optical bistability, and the generation of nonclassical states of light [21]. For Kerr medium, the nonlinear interaction Hamiltonian is written as

$$\hat{H}_K = \hbar\chi \left(\hat{a}^\dagger \hat{a} + \hat{b}^\dagger \hat{b}\right)^2. \tag{6}$$

where χ denotes the Kerr nonlinear coupling coefficient and $\hat{a}^\dagger\hat{a}$ and $\hat{b}^\dagger\hat{b}$ are the photon-number operators for cavity modes a and b, respectively. The square of the total photon-number operator can be expanded algebraically as

$$\left(\hat{a}^\dagger\hat{a}+\hat{b}^\dagger\hat{b}\right)^2=(\hat{a}^\dagger\hat{a})^2+(\hat{b}^\dagger\hat{b})^2+2\hat{a}^\dagger\hat{a}\hat{b}^\dagger\hat{b}.$$

Substituting this result into Eq.6, the Kerr Hamiltonian gives

$$\hat{H}_K=\hbar\chi\Big[(\hat{a}^\dagger\hat{a})^2+(\hat{b}^\dagger\hat{b})^2+2\hat{a}^\dagger\hat{a}\hat{b}^\dagger\hat{b}\Big]. \tag{7}$$

The first two terms represent self-phase modulation, whereas the last term corresponds to cross-phase modulation and is responsible for enhancing the correlations between the two cavity modes. The last term $2\hat{a}^\dagger\hat{a}\hat{b}^\dagger\hat{b}$ is the cross-Kerr interaction responsible for enhancing intermode correlations and entanglement. The complete Hamiltonian of the atom cavity system is

$$\begin{aligned}\hat{H}=&\sum_{i=1}^{3}\hbar\omega_i|i\rangle\langle i|+\hbar\omega_a\hat{a}^\dagger\hat{a}+\hbar\omega_b\hat{b}^\dagger\hat{b}+\hbar g_a(\hat{a}\hat{\sigma}_{32}+\hat{a}^\dagger\hat{\sigma}_{23})+\hbar g_b(\hat{b}\hat{\sigma}_{21}+\hat{b}^\dagger\hat{\sigma}_{12})\\&+\frac{\hbar\Omega_p}{2}(\hat{\sigma}_{31}+\hat{\sigma}_{13})+\hbar\chi(\hat{a}^\dagger\hat{a}+\hat{b}^\dagger\hat{b})^2.\end{aligned} \tag{8}$$

This Hamiltonian completely specifies the coherent dynamics of the three-level laser system. The interaction picture transformation is defined by

$$\hat{O}_I(t)=e^{\frac{i\hat{H}_0t}{\hbar}}\hat{O}_Se^{-\frac{i\hat{H}_0t}{\hbar}},$$

where $\hat{O}_S$ and $\hat{O}_I$ denote the Schrödinger and interaction-picture operators [20], respectively.

The interaction Hamiltonian is then

$$\hat{H}_I=e^{\frac{i\hat{H}_0t}{\hbar}}(\hat{H}-\hat{H}_0)e^{-\frac{i\hat{H}_0t}{\hbar}}.$$

Evaluating this transformation introduces oscillating phase factors such as

$$e^{-i(\omega_{32}-\omega_a)t},\quad e^{-i(\omega_{21}-\omega_b)t},\quad e^{-i(\omega_{31}-\omega_p)t},$$

which represent the detuning between the atomic transitions and the corresponding driving fields [21].

For resonant operation, we impose the conditions

$$\omega_{32}=\omega_a,\quad \omega_{21}=\omega_b,\quad \omega_{31}=\omega_p.$$

Under these exact resonance conditions, all rapidly oscillating exponential factors become unity. As a result, the interaction Hamiltonian reduces to

$$\begin{aligned}\hat{H}_I =&\hbar g_a(\hat{a}\hat{\sigma}_{32} + \hat{a}^\dagger\hat{\sigma}_{23}) + \hbar g_b(\hat{b}\hat{\sigma}_{21} + \hat{b}^\dagger\hat{\sigma}_{12}) \\ &+ \frac{\hbar\Omega_p}{2}(\hat{\sigma}_{31} + \hat{\sigma}_{13}) + \hbar\chi(\hat{a}^\dagger\hat{a} + \hat{b}^\dagger\hat{b})^2.\end{aligned} \tag{9}$$

This interaction Hamiltonian contains only the terms responsible for the coherent evolution of the coupled atom-cavity system.

2.1 Master Equation and Heisenberg Langevin Dynamics

In the interaction picture, the time evolution of the density operator is governed by the master equation described by the density operator $\hat{\rho}$. After applying the Born and Markov approximations [22] and tracing over the reservoir degrees of freedom [23], the complete master equation therefore becomes

$$\frac{d\hat{\rho}}{dt} = -\frac{i}{\hbar}\left[\hat{H}_I, \hat{\rho}\right] + \mathcal{L}_A\hat{\rho} + \mathcal{L}_C\hat{\rho} + \mathcal{L}_{\text{sq}}\hat{\rho}, \tag{10}$$

where $\hat{H}_I$ is the interaction Hamiltonian given by Eq. 9. The first term in Eq.(10) describes the coherent evolution generated by the atom field interaction, coherent pumping, and Kerr nonlinearity.

Using the standard Lindblad dissipator [24],

$$\mathcal{D}[\hat{C}]\hat{\rho} = 2\hat{C}\hat{\rho}\hat{C}^\dagger - \hat{C}^\dagger\hat{C}\hat{\rho} - \hat{\rho}\hat{C}^\dagger\hat{C}, \tag{11}$$

the spontaneous emission contribution becomes

$$\mathcal{L}_{\text{atom}}\hat{\rho} = \frac{\gamma_{32}}{2}\mathcal{D}[\hat{\sigma}_{23}]\hat{\rho} + \frac{\gamma_{21}}{2}\mathcal{D}[\hat{\sigma}_{12}]\hat{\rho}. \tag{12}$$

Expanding the dissipators gives

$$\mathcal{L}_{\text{atom}}\hat{\rho} = \frac{\gamma_{32}}{2}\left(2\hat{\sigma}_{23}\hat{\rho}\hat{\sigma}_{32} - \hat{\sigma}_{33}\hat{\rho} - \hat{\rho}\hat{\sigma}_{33}\right) + \frac{\gamma_{21}}{2}\left(2\hat{\sigma}_{12}\hat{\rho}\hat{\sigma}_{21} - \hat{\sigma}_{22}\hat{\rho} - \hat{\rho}\hat{\sigma}_{22}\right). \tag{13}$$

where γ_{32} and γ_{21} are the spontaneous emission rates of the transitions $|3\rangle \to |2\rangle$ and $|2\rangle \to |1\rangle$, respectively. The first term describes quantum jumps associated with spontaneous photon emission, while the remaining terms ensure proper normalization and preserve complete positivity.

The cavity damping can also be described using the Lindblad formalism [26]. The cavity damping Liouvillian becomes

$$\mathcal{L}_{\text{cav}}\hat{\rho} = \frac{\kappa_a}{2}\mathcal{D}[\hat{a}]\hat{\rho} + \frac{\kappa_b}{2}\mathcal{D}[\hat{b}]\hat{\rho}, \tag{14}$$

Expanding the Lindblad dissipators yields

$$\mathcal{L}_{\text{cav}}\hat{\rho} = \frac{\kappa_a}{2}\left(2\hat{a}\hat{\rho}\hat{a}^\dagger - \hat{a}^\dagger\hat{a}\hat{\rho} - \hat{\rho}\hat{a}^\dagger\hat{a}\right) + \frac{\kappa_b}{2}\left(2\hat{b}\hat{\rho}\hat{b}^\dagger - \hat{b}^\dagger\hat{b}\hat{\rho} - \hat{\rho}\hat{b}^\dagger\hat{b}\right). \tag{15}$$

where κ_a and κ_b denote the damping rates of cavity modes a and b, respectively. The statistical properties of the squeezed reservoir are completely characterized by the squeezing parameter r and the squeezing phase ϕ [20]. The corresponding reservoir parameters are

$$N = \sinh^2 r, \tag{16}$$

which represents the average photon number of the squeezed vacuum, and

$$M = \sinh r \cosh r e^{i\phi} = \sqrt{N(N+1)}e^{i\phi}, \tag{17}$$

which quantifies the two-photon correlations generated by the squeezed field [27].

The interaction between cavity mode a and the squeezed reservoir can be described using the generalized Lindblad master equation for squeezed states. The corresponding Liouvillian is

$$\begin{aligned}\mathcal{L}_{\text{sq}}^{(a)}\hat{\rho} =& \frac{\kappa_a}{2}(N+1)\left(2a\hat{\rho}a^\dagger - a^\dagger a\hat{\rho} - \hat{\rho}a^\dagger a\right) + \frac{\kappa_a}{2}N\left(2a^\dagger\hat{\rho}a - aa^\dagger\hat{\rho} - \hat{\rho}aa^\dagger\right) \\ &- \frac{\kappa_a}{2}M\left(2a\hat{\rho}a - aa\hat{\rho} - \hat{\rho}aa\right) - \frac{\kappa_a}{2}M^*\left(2a^\dagger\hat{\rho}a^\dagger - a^\dagger a^\dagger\hat{\rho} - \hat{\rho}a^\dagger a^\dagger\right).\end{aligned} \tag{18}$$

The first two terms correspond to ordinary photon absorption and emission processes, modified by the nonzero thermal occupation. The last two terms originate exclusively from the squeezed nature of the reservoir and describe correlated two-photon absorption and emission processes.

Similarly, for mode b,

$$\begin{aligned}\mathcal{L}_{\text{sq}}^{(b)}\hat{\rho} =& \frac{\kappa_b}{2}(N+1)\left(2b\hat{\rho}b^\dagger - b^\dagger b\hat{\rho} - \hat{\rho}b^\dagger b\right) + \frac{\kappa_b}{2}N\left(2b^\dagger\hat{\rho}b - bb^\dagger\hat{\rho} - \hat{\rho}bb^\dagger\right) \\ &- \frac{\kappa_b}{2}M\left(2b\hat{\rho}b - bb\hat{\rho} - \hat{\rho}bb\right) - \frac{\kappa_b}{2}M^*\left(2b^\dagger\hat{\rho}b^\dagger - b^\dagger b^\dagger\hat{\rho} - \hat{\rho}b^\dagger b^\dagger\right).\end{aligned} \tag{19}$$

The total squeezed vacuum contribution for identical cavity damping rates, $\kappa_a = \kappa_b = \kappa$, the squeezed-reservoir Liouvillian can be written compactly as

$$\begin{aligned}\frac{d\hat{\rho}}{dt} =& -\frac{i}{\hbar}\Big[\hbar g_a\left(\hat{a}\hat{\sigma}_{32} + \hat{a}^\dagger\hat{\sigma}_{23}\right) + \hbar g_b\left(\hat{b}\hat{\sigma}_{21} + \hat{b}^\dagger\hat{\sigma}_{12}\right) + \frac{\hbar\Omega_p}{2}\left(\hat{\sigma}_{31} + \hat{\sigma}_{13}\right) + \hbar\chi\left(\hat{a}^\dagger\hat{a} + \hat{b}^\dagger\hat{b}\right)^2, \hat{\rho}\Big] \\ &+ \frac{\gamma_{32}}{2}\left(2\hat{\sigma}_{23}\hat{\rho}\hat{\sigma}_{32} - \hat{\sigma}_{33}\hat{\rho} - \hat{\rho}\hat{\sigma}_{33}\right) + \frac{\gamma_{21}}{2}\left(2\hat{\sigma}_{12}\hat{\rho}\hat{\sigma}_{21} - \hat{\sigma}_{22}\hat{\rho} - \hat{\rho}\hat{\sigma}_{22}\right) + \frac{\kappa_a}{2}\left(2\hat{a}\hat{\rho}\hat{a}^\dagger - \hat{a}^\dagger\hat{a}\hat{\rho} - \hat{\rho}\hat{a}^\dagger\hat{a}\right) \\ &+ \frac{\kappa_a}{2}(N+1)\left(2\hat{a}\hat{\rho}\hat{a}^\dagger - \hat{a}^\dagger\hat{a}\hat{\rho} - \hat{\rho}\hat{a}^\dagger\hat{a}\right) + \frac{\kappa_a}{2}N\left(2\hat{a}^\dagger\hat{\rho}\hat{a} - \hat{a}\hat{a}^\dagger\hat{\rho} - \hat{\rho}\hat{a}\hat{a}^\dagger\right) - \frac{\kappa_a}{2}M\left(2\hat{a}\hat{\rho}\hat{a} - \hat{a}\hat{a}\hat{\rho} - \hat{\rho}\hat{a}\hat{a}\right) \\ &- \frac{\kappa_a}{2}M^*\left(2\hat{a}^\dagger\hat{\rho}\hat{a}^\dagger - \hat{a}^\dagger\hat{a}^\dagger\hat{\rho} - \hat{\rho}\hat{a}^\dagger\hat{a}^\dagger\right) + \frac{\kappa_b}{2}(N+1)\left(2\hat{b}\hat{\rho}\hat{b}^\dagger - \hat{b}^\dagger\hat{b}\hat{\rho} - \hat{\rho}\hat{b}^\dagger\hat{b}\right) + \frac{\kappa_b}{2}N\left(2\hat{b}^\dagger\hat{\rho}\hat{b} - \hat{b}\hat{b}^\dagger\hat{\rho} - \hat{\rho}\hat{b}\hat{b}^\dagger\right) \\ &- \frac{\kappa_b}{2}M\left(2\hat{b}\hat{\rho}\hat{b} - \hat{b}\hat{b}\hat{\rho} - \hat{\rho}\hat{b}\hat{b}\right) - \frac{\kappa_b}{2}M^*\left(2\hat{b}^\dagger\hat{\rho}\hat{b}^\dagger - \hat{b}^\dagger\hat{b}^\dagger\hat{\rho} - \hat{\rho}\hat{b}^\dagger\hat{b}^\dagger\right).\end{aligned} \tag{20}$$

Using Eqs. (13), (15), and (20), substitute the interaction Hamiltonian, the atomic Liouvillian, the cavity damping Liouvillian and the squeezed-reservoir Liouvillian into Eq. (10) yields

$$\begin{aligned}\frac{d\hat{\rho}}{dt} =& -\frac{i}{\hbar}\left[\hbar g_a\left(\hat{a}\hat{\sigma}_{32}+\hat{a}^\dagger\hat{\sigma}_{23}\right)+\hbar g_b\left(\hat{b}\hat{\sigma}_{21}+\hat{b}^\dagger\hat{\sigma}_{12}\right)+\frac{\hbar\Omega_p}{2}\left(\hat{\sigma}_{31}+\hat{\sigma}_{13}\right)+\hbar\chi\left(\hat{a}^\dagger\hat{a}+\hat{b}^\dagger\hat{b}\right)^2,\hat{\rho}\right]\\
&+\frac{\gamma_{32}}{2}\left(2\hat{\sigma}_{23}\hat{\rho}\hat{\sigma}_{32}-\hat{\sigma}_{33}\hat{\rho}-\hat{\rho}\hat{\sigma}_{33}\right)+\frac{\gamma_{21}}{2}\left(2\hat{\sigma}_{12}\hat{\rho}\hat{\sigma}_{21}-\hat{\sigma}_{22}\hat{\rho}-\hat{\rho}\hat{\sigma}_{22}\right)\\
&+\frac{\kappa_a}{2}\left(2\hat{a}\hat{\rho}\hat{a}^\dagger-\hat{a}^\dagger\hat{a}\hat{\rho}-\hat{\rho}\hat{a}^\dagger\hat{a}\right)+\frac{\kappa_b}{2}\left(2\hat{b}\hat{\rho}\hat{b}^\dagger-\hat{b}^\dagger\hat{b}\hat{\rho}-\hat{\rho}\hat{b}^\dagger\hat{b}\right)+\frac{\kappa_a}{2}(N+1)\left(2\hat{a}\hat{\rho}\hat{a}^\dagger-\hat{a}^\dagger\hat{a}\hat{\rho}-\hat{\rho}\hat{a}^\dagger\hat{a}\right)\\
&+\frac{\kappa_a}{2}N\left(2\hat{a}^\dagger\hat{\rho}\hat{a}-\hat{a}\hat{a}^\dagger\hat{\rho}-\hat{\rho}\hat{a}\hat{a}^\dagger\right)-\frac{\kappa_a}{2}M\left(2\hat{a}\hat{\rho}\hat{a}-\hat{a}\hat{a}\hat{\rho}-\hat{\rho}\hat{a}\hat{a}\right)\\
&-\frac{\kappa_a}{2}M^*\left(2\hat{a}^\dagger\hat{\rho}\hat{a}^\dagger-\hat{a}^\dagger\hat{a}^\dagger\hat{\rho}-\hat{\rho}\hat{a}^\dagger\hat{a}^\dagger\right)+\frac{\kappa_b}{2}(N+1)\left(2\hat{b}\hat{\rho}\hat{b}^\dagger-\hat{b}^\dagger\hat{b}\hat{\rho}-\hat{\rho}\hat{b}^\dagger\hat{b}\right)\\
&+\frac{\kappa_b}{2}N\left(2\hat{b}^\dagger\hat{\rho}\hat{b}-\hat{b}\hat{b}^\dagger\hat{\rho}-\hat{\rho}\hat{b}\hat{b}^\dagger\right)-\frac{\kappa_b}{2}M\left(2\hat{b}\hat{\rho}\hat{b}-\hat{b}\hat{b}\hat{\rho}-\hat{\rho}\hat{b}\hat{b}\right)-\frac{\kappa_b}{2}M^*\left(2\hat{b}^\dagger\hat{\rho}\hat{b}^\dagger-\hat{b}^\dagger\hat{b}^\dagger\hat{\rho}-\hat{\rho}\hat{b}^\dagger\hat{b}^\dagger\right)\end{aligned}$$

2.2 Linearized Stochastic Equations

Instead of following the evolution of the density operator, the Heisenberg picture follows the evolution of the operators themselves while the quantum state remains fixed. The expectation value of an arbitrary system operator $\hat{O}$ [28] is defined as

$$\langle\hat{O}\rangle = \mathrm{Tr}(\hat{O}\hat{\rho}). \tag{21}$$

Differentiating both sides with respect to time gives

$$\frac{d}{dt}\langle\hat{O}\rangle = \mathrm{Tr}\left(\hat{O}\frac{d\hat{\rho}}{dt}\right), \tag{22}$$

where the time dependence of $\hat{\rho}$ is determined by the master equation.

Substituting the complete master equation,

$$\frac{d\hat{\rho}}{dt} = -\frac{i}{\hbar}[\hat{H}_I,\hat{\rho}] + \mathcal{L}_{\mathrm{atom}}\hat{\rho} + \mathcal{L}_{\mathrm{cav}}\hat{\rho} + \mathcal{L}_{\mathrm{sq}}\hat{\rho}, \tag{23}$$

yields

$$\frac{d}{dt}\langle\hat{O}\rangle = -\frac{i}{\hbar}\mathrm{Tr}\left(\hat{O}[\hat{H}_I,\hat{\rho}]\right) + \mathrm{Tr}\left(\hat{O}\mathcal{L}_{\mathrm{atom}}\hat{\rho}\right) + \mathrm{Tr}\left(\hat{O}\mathcal{L}_{\mathrm{cav}}\hat{\rho}\right) + \mathrm{Tr}\left(\hat{O}\mathcal{L}_{\mathrm{sq}}\hat{\rho}\right). \tag{24}$$

The first term describes coherent evolution generated by the interaction Hamiltonian, whereas the remaining three terms account for dissipative processes arising from spontaneous emission, cavity losses, and the squeezed vacuum reservoir. To derive the

equation of motion for cavity mode a, the coherent contribution is

$$\frac{i}{\hbar}[\hat{H}_I, \hat{a}]. \tag{25}$$

Using

$$[\hat{a}, \hat{a}^\dagger] = 1, \quad [\hat{a}, \hat{b}] = 0, \tag{26}$$

we obtain

$$[\hat{H}_{AF}, \hat{a}] = -\hbar g_a \hat{\sigma}_{23}. \tag{27}$$

Therefore,

$$\left(\frac{d\hat{a}}{dt}\right)_{AF} = -g_a \hat{\sigma}_{23}. \tag{28}$$

This term describes the exchange of excitation between the cavity mode and the atomic transition $|3\rangle \longrightarrow |2\rangle$. Introducing the total photon number operator

$$\hat{N} = \hat{a}^\dagger \hat{a} + \hat{b}^\dagger \hat{b}, \tag{29}$$

the Kerr Hamiltonian becomes

$$\hat{H}_K = \hbar \chi \hat{N}^2. \tag{30}$$

Using the commutator identity

$$[\hat{N}, \hat{a}] = -\hat{a}, \tag{31}$$

one finds

$$[\hat{N}^2, \hat{a}] = -2\hat{N}\hat{a}. \tag{32}$$

Hence,

$$[\hat{H}_K, \hat{a}] = -2\hbar\chi(\hat{a}^\dagger \hat{a} + \hat{b}^\dagger \hat{b})\hat{a}. \tag{33}$$

Therefore,

$$\left(\frac{d\hat{a}}{dt}\right)_K = -i2\chi(\hat{a}^\dagger \hat{a} + \hat{b}^\dagger \hat{b})\hat{a}. \tag{34}$$

This nonlinear term produces an intensity dependent phase shift and couples the evolution of each cavity mode to the total intracavity photon number. Applying the cavity damping Liouvillian to the annihilation operator yields

$$\left(\frac{d\hat{a}}{dt}\right)_{\text{loss}} = -\frac{\kappa}{2}\hat{a}. \tag{35}$$

This term represents the exponential decay of the cavity field due to photon leakage through the mirrors. These fluctuations are incorporated through the Langevin noise operator $\hat{F}_a(t)$ [**?**], whose statistical properties are determined by the reservoir correlation functions. Combining all coherent and dissipative contributions gives

$$\frac{d\hat{a}}{dt} = -g_a \hat{\sigma}_{23} - i2\chi(\hat{a}^\dagger \hat{a} + \hat{b}^\dagger \hat{b})\hat{a} - \frac{\kappa}{2}\hat{a} + \hat{F}_a(t). \tag{36}$$

This is the Heisenberg Langevin equation governing the evolution of cavity mode a. Following exactly the same procedure for cavity mode b, the atom field interaction contributes

$$\left(\frac{d\hat{b}}{dt}\right)_{AF} = -g_b\hat{\sigma}_{12}. \tag{37}$$

The Kerr nonlinearity contributes

$$\left(\frac{d\hat{b}}{dt}\right)_{K} = -i2\chi(\hat{a}^\dagger\hat{a} + \hat{b}^\dagger\hat{b})\hat{b}. \tag{38}$$

The cavity damping contributes

$$\left(\frac{d\hat{b}}{dt}\right)_{\text{loss}} = -\frac{\kappa}{2}\hat{b}. \tag{39}$$

Finally, the Langevin noise operator associated with the squeezed reservoir is denoted by $\hat{F}_b(t)$.

Combining all terms yields

$$\frac{d\hat{b}}{dt} = -g_b\hat{\sigma}_{12} - i2\chi(\hat{a}^\dagger\hat{a} + \hat{b}^\dagger\hat{b})\hat{b} - \frac{\kappa}{2}\hat{b} + \hat{F}_b(t). \tag{40}$$

As a result, in the good-cavity regime ($\gamma_{32}, \gamma_{21} \gg \kappa$) [29] the atomic subsystem reaches its steady state much faster than the cavity field evolves. The Heisenberg equation of motion for any atomic operator [31] is

$$\frac{d\hat{\sigma}_{ij}}{dt} = \frac{i}{\hbar}[\hat{H}_I, \hat{\sigma}_{ij}] + \mathcal{L}^\dagger(\hat{\sigma}_{ij}), \tag{41}$$

where the first term describes coherent atom field interaction and the second term represents spontaneous emission.

Applying this equation to the atomic coherence operator $\hat{\sigma}_{23}$ gives

$$\frac{d\hat{\sigma}_{23}}{dt} = -\frac{\gamma_{32}}{2}\hat{\sigma}_{23} + ig_a\hat{a}(\hat{\sigma}_{33} - \hat{\sigma}_{22}) + i\frac{\Omega_p}{2}\hat{\sigma}_{21} + \hat{F}_{23}(t), \tag{42}$$

where $\hat{F}_{23}(t)$ denotes the associated Langevin noise operator.

Similarly,

$$\frac{d\hat{\sigma}_{12}}{dt} = -\frac{\gamma_{21}}{2}\hat{\sigma}_{12} + ig_b\hat{b}(\hat{\sigma}_{22} - \hat{\sigma}_{11}) + i\frac{\Omega_p}{2}\hat{\sigma}_{32} + \hat{F}_{12}(t). \tag{43}$$

These equations explicitly show that the two atomic coherences are coupled through the coherent pump field.

The coupled linear equations can be solved using straightforward algebraic elimination [30]. Eliminating $\hat{\sigma}_{21}$ and $\hat{\sigma}_{32}$ leads to expressions that depend only on the cavity-field operators.

The resulting steady state solutions can be written in the compact form

$$\hat{\sigma}_{23} = A\hat{a} + B\hat{b}^{\dagger}, \tag{44}$$

$$\hat{\sigma}_{12} = C\hat{b} + D\hat{a}^{\dagger}. \tag{45}$$

The coefficients A, B, C, and D are determined by the spontaneous emission rates, atom field coupling strengths, and coherent pump. Symbolically,

$$A = A(g_a, \Omega_p, \gamma_{32}), \tag{46}$$

$$B = B(g_a, g_b, \Omega_p, \gamma_{21}, \gamma_{32}), \tag{47}$$

$$C = C(g_b, \Omega_p, \gamma_{21}), \tag{48}$$

$$D = D(g_a, g_b, \Omega_p, \gamma_{21}, \gamma_{32}). \tag{49}$$

Substituting the steady state atomic coherences into the Heisenberg Langevin equations gives

$$\frac{d\hat{a}}{dt} = -g_a(A\hat{a} + B\hat{b}^{\dagger}) - i2\chi(\hat{a}^{\dagger}\hat{a} + \hat{b}^{\dagger}\hat{b})\hat{a} - \frac{\kappa}{2}\hat{a} + \hat{F}_a(t), \tag{50}$$

$$\frac{d\hat{b}}{dt} = -g_b(C\hat{b} + D\hat{a}^{\dagger}) - i2\chi(\hat{a}^{\dagger}\hat{a} + \hat{b}^{\dagger}\hat{b})\hat{b} - \frac{\kappa}{2}\hat{b} + \hat{F}_b(t). \tag{51}$$

Introducing the effective coefficients

$$\mu_a = g_a A + \frac{\kappa}{2}, \quad \mu_b = g_b C + \frac{\kappa}{2}, \tag{52}$$

$$\nu_a = -g_a B, \quad \nu_b = -g_b D, \tag{53}$$

the equations reduce to the compact form

$$\frac{d\hat{a}}{dt} = -\mu_a\hat{a} + \nu_a\hat{b}^{\dagger} - i2\chi(\hat{a}^{\dagger}\hat{a} + \hat{b}^{\dagger}\hat{b})\hat{a} + \hat{F}_a(t), \tag{54}$$

$$\frac{d\hat{b}}{dt} = -\mu_b\hat{b} + \nu_b\hat{a}^{\dagger} - i2\chi(\hat{a}^{\dagger}\hat{a} + \hat{b}^{\dagger}\hat{b})\hat{b} + \hat{F}_b(t). \tag{55}$$

These shows the competition between effective damping (μ_a, μ_b), gain and intermode coupling (ν_a, ν_b), Kerr nonlinearity, and quantum noise.

Since the normal ordering of field operators is assumed throughout this work, we employ the positive P representation, in which operator expectation values are replaced by stochastic averages over complex variables [32].

$$\alpha(t) \longrightarrow \hat{a}, \qquad \beta(t) \longrightarrow \hat{b}, \tag{56}$$

Thus,

$$\langle \hat{a}^\dagger \hat{a} \rangle = \langle \alpha^* \alpha \rangle_s, \langle \hat{b}^\dagger \hat{b} \rangle = \langle \beta^* \beta \rangle_s, \tag{57}$$

Replacing the field operators by their corresponding stochastic amplitudes, the effective Langevin equations become

$$\frac{d\alpha}{dt} = -\mu_a \alpha + \nu_a \beta^* - i2\chi(|\alpha|^2 + |\beta|^2)\alpha + f_a(t), \tag{58}$$

$$\frac{d\beta}{dt} = -\mu_b \beta + \nu_b \alpha^* - i2\chi(|\alpha|^2 + |\beta|^2)\beta + f_b(t), \tag{59}$$

where $f_a(t)$ and $f_b(t)$ are complex Gaussian noise functions originating from the quantum fluctuations of the squeezed reservoir [33].

For a squeezed vacuum reservoir characterized by the squeezing parameter r, the noise correlation functions satisfy

$$\begin{aligned}
\langle f_\alpha(t) f_\alpha^*(t') \rangle &= \kappa(N+1)\delta(t-t'), \\
\langle f_\alpha^*(t) f_\alpha(t') \rangle &= \kappa N \delta(t-t'), \\
\langle f_\alpha(t) f_\alpha(t') \rangle &= -\kappa M \delta(t-t'), \\
\langle f_\alpha^*(t) f_\alpha^*(t') \rangle &= -\kappa M^* \delta(t-t'),
\end{aligned} \tag{60}$$

Similar relations hold for mode b. Using Itô calculus on the linearized stochastic differential equations [34], the equations of motion for these moments are obtained as:

$$\frac{d}{dt}\langle \alpha^\dagger \alpha \rangle = -2\mu_a \langle \alpha^\dagger \alpha \rangle + \nu_a \langle \alpha \beta \rangle + \nu_a \langle \alpha^\dagger \beta^\dagger \rangle + \kappa N, \tag{61}$$

$$\frac{d}{dt}\langle \beta^\dagger \beta \rangle = -2\mu_b \langle \beta^\dagger \beta \rangle + \nu_b \langle \alpha \beta \rangle + \nu_b \langle \alpha^\dagger \beta^\dagger \rangle + \kappa N, \tag{62}$$

$$\frac{d}{dt}\langle \alpha \beta \rangle = -(\mu_a + \mu_b)\langle \alpha \beta \rangle + \nu_a \langle \beta^\dagger \beta \rangle + \nu_b \langle \alpha^\dagger \alpha \rangle + \kappa M. \tag{63}$$

At steady state,

$$\frac{d}{dt}\langle \alpha^\dagger \alpha \rangle = \frac{d}{dt}\langle \beta^\dagger \beta \rangle = \frac{d}{dt}\langle \alpha \beta \rangle = 0. \tag{64}$$

Hence, the steady-state equations become

$$2\mu_a \langle \alpha^\dagger \alpha \rangle = \nu_a \left(\langle \alpha \beta \rangle + \langle \alpha^\dagger \beta^\dagger \rangle \right) + \kappa N, \tag{65}$$

$$2\mu_b \langle \beta^\dagger \beta \rangle = \nu_b \left(\langle \alpha \beta \rangle + \langle \alpha^\dagger \beta^\dagger \rangle \right) + \kappa N, \tag{66}$$

$$(\mu_a + \mu_b)\langle \alpha \beta \rangle = \nu_a \langle \beta^\dagger \beta \rangle + \nu_b \langle \alpha^\dagger \alpha \rangle + \kappa M. \tag{67}$$

We define the steady state shorthand notation for the photon numbers and intermode correlations as:

$$n_a = \langle a^\dagger a \rangle, \quad n_b = \langle b^\dagger b \rangle, \quad m = \langle ab \rangle. \tag{68}$$

At steady state, setting the time derivatives to zero

$$\frac{dn_a}{dt} = \frac{dn_b}{dt} = \frac{dm}{dt} = 0$$

the equations simplify to:

$$\begin{aligned} 2\mu_a n_a &= \nu_a(m+m^*) + \kappa N \\ 2\mu_b n_b &= \nu_b(m+m^*) + \kappa N \\ (\mu_a+\mu_b)m &= \nu_a n_b + \nu_b n_a + \kappa M. \end{aligned} \tag{69}$$

Assuming exact resonance and real correlations such that $m = m^*$, the steady-state photon numbers can be expressed explicitly as:

$$n_a = \frac{2\nu_a m + \kappa N}{2\mu_a}, \tag{70}$$

$$n_b = \frac{2\nu_b m + \kappa N}{2\mu_b}. \tag{71}$$

Substituting these expressions back into the total correlation equation yields the explicit closed-form solution for m:

$$m = \frac{\kappa N\left(\frac{\nu_a}{2\mu_b} + \frac{\nu_b}{2\mu_a}\right) + \kappa M}{(\mu_a+\mu_b) - \nu_a\nu_b\left(\frac{1}{\mu_a} + \frac{1}{\mu_b}\right)}. \tag{72}$$

The total variance of the EPR type quadrature operators $\hat{u}$ and $\hat{v}$ is given by [34],

$$D = \Delta u^2 + \Delta v^2. \tag{73}$$

For zero-mean fluctuations, this parameter simplifies in terms of our second-order moments to:

$$D = 4 + 2(n_a + n_b) - 4\mathrm{Re}(m). \tag{74}$$

The cavity modes exhibit nonclassical bipartite entanglement whenever $D < 4$.

$$\begin{aligned} D =& 4 + \kappa N\left(\frac{1}{\mu_a} + \frac{1}{\mu_b}\right) + \left[2\left(\frac{\nu_a}{\mu_a} + \frac{\nu_b}{\mu_b}\right) - 4\right] \\ & \frac{\kappa N\left(\frac{\nu_a}{2\mu_b} + \frac{\nu_b}{2\mu_a}\right) + \kappa M}{(\mu_a+\mu_b) - \nu_a\nu_b\left(\frac{1}{\mu_a} + \frac{1}{\mu_b}\right)}. \end{aligned} \tag{75}$$

The cavity modes are entangled whenever the Duan criterion satisfies $D < 4$ [8]. Therefore, increasing the Kerr nonlinearity χ and the squeezing parameter r enhances the intermode correlation m, reduces the Duan parameter D, and consequently strengthens the bipartite entanglement generated by the three-level laser system [2, 35].

3 Numerical Results and Discussion

The steady state solutions from the linearized Langevin equations were computed numerically by applying the analytical formulas created in the previous sections.

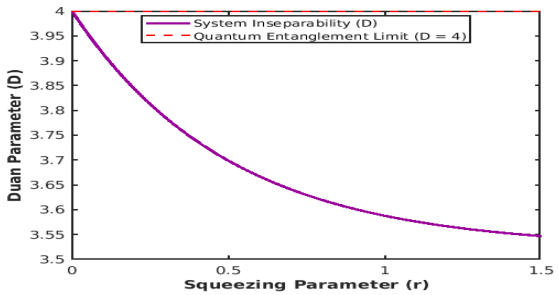


Figure 2

Figure 2 shows how the Duan inseparability parameter changes with the squeezing parameter of the squeezed vacuum reservoir. The results show that when the squeezing parameter increases at first, the Duan parameter decreases, which means there is a big improvement in continuous variable bipartite entanglement between the two cavity modes. So, when the Duan parameter drops below this value, it confirms that there are strong quantum correlations inside the laser cavity. As the squeezing parameter gets larger, the cavity modes become more entangled because the squeezed reservoir makes the phase sensitive correlations stronger, which helps create two mode quantum coherence. Additionally, the squeezed vacuum reservoir greatly enhance the bipartite entanglement between the two cavity modes with cascade atomic coherence and Kerr nonlinearity, it allows for the effective generation of strongly entangled nonclassical light. Figure 3 shows how the Duan inseparability parameter depends on the Kerr

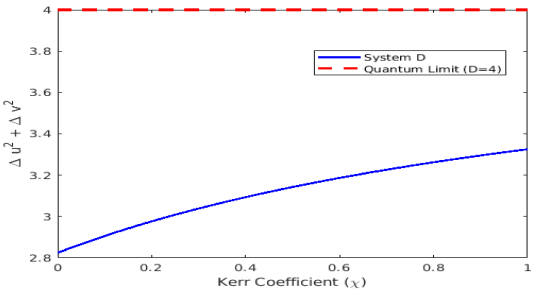


Figure 3

nonlinear coefficient χ. The numerical results clearly show that as the Kerr coefficient increases, the Duan parameter decreases continuously.This shows that the Kerr nonlinear medium is important for improving continuous-variable bipartite entanglement inside the cavity. As the Kerr coefficient gets larger, this nonlinear effect becomes stronger, causing the fluctuations between the two modes to become more correlated and the intermode correlation function $\langle ab \rangle$ to increase steadily [36]. Since the cascade atomic transitions already create strong correlations between the photon numbers in the two modes, the Kerr-induced phase modulation helps to make their quantum fluctuations more synchronized, and reduces random phase diffusion that could otherwise reduce the entanglement. Thus, Figure 3 shows that the Kerr nonlinear medium improves continuous-variable bipartite entanglement by increasing the nonlinear interaction and the quantum correlations between the two cavity modes. Figure 4 show

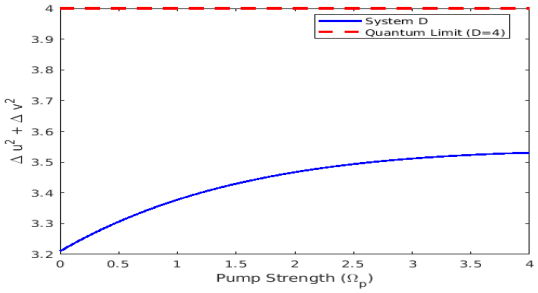


Figure 4

how the Duan inseparability parameter changes with the coherent pump strength Ω_p. The numerical results show that the coherent pump field plays a major role in creating continuous-variable bipartite entanglement in the three-level laser system. As the pump strength increases from a low level, the Duan parameter steadily decreases, which means the produced radiation becomes increasingly entangled. This happens because a higher pump strength improves the intermode correlation function $\langle ab \rangle$, which in turn lowers the Duan inseparability parameter for enhancing atomic coherence, improving intermode correlations, and encouraging the production of correlated photon pairs. Figure 5 shows how the total number of photons inside the cavity, which is the sum of $\langle \hat{n}_a \rangle$ and $\langle \hat{n}_b \rangle$, changes with the squeezing parameter r of the squeezed vacuum reservoir. The results show that as the squeezing parameter increases, so does the total number of photons inside the cavity. Since the photons from the squeezed vacuum are created in pairs that are strongly correlated, the increase in photon number also means more of these correlated pairs are available. So, the squeezed vacuum reservoir not only increases the number of photons in the cavity but also greatly improves the creation of continuous variable entanglement between the two cavity modes.

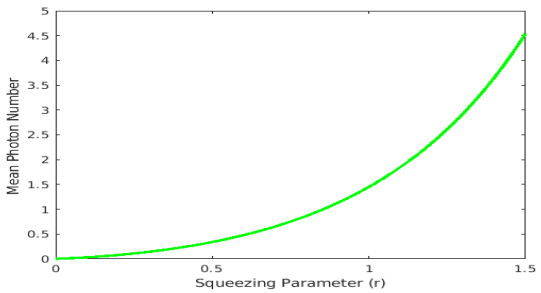


Figure 5

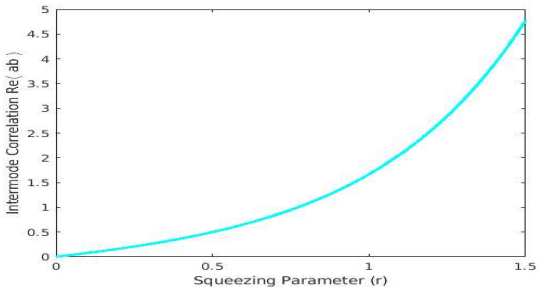


Figure 6

Figure 6 shows how the real part of the intermode correlation function, $Re\langle ab\rangle$, changes with the squeezing parameter r of the squeezed vacuum reservoir.The intermode correlation is a key measurement in continuous-variable quantum optics because it directly shows how coherent the two cavity modes are [37].The results show that $Re\langle ab\rangle$ steadily increases as the squeezing parameter increases, meaning that more squeezing leads to better generation of correlated photon pairs within the optical cavity.As the squeezing parameter rises, the reservoir correlation parameter M also rises quickly, allowing the squeezed vacuum reservoir to send stronger phase-sensitive quantum correlations to the field inside the cavity, which in turn enhances continuous-variable bipartite entanglement. Figure 7 shows a three-dimensional surface plot of the Duan inseparability parameter, which depends on the squeezing parameter r and the Kerr nonlinear coefficient χ. The numerical results show that as either the squeezing parameter or the Kerr coefficient increases, the Duan parameter decreases steadily. The squeezed vacuum reservoir improves entanglement by sending strongly correlated photon pairs into the cavity, which increases the number of squeezed photons and the phase-sensitive correlation parameter. Thus, Figure 7 clearly shows that the squeezed vacuum reservoir and the Kerr nonlinear medium work together to enhance

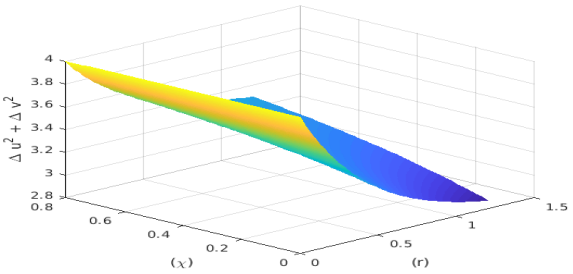


Figure 7

continuous-variable bipartite entanglement, with the strongest entanglement occurring when both the squeezing parameter and the Kerr coefficient are large. The results

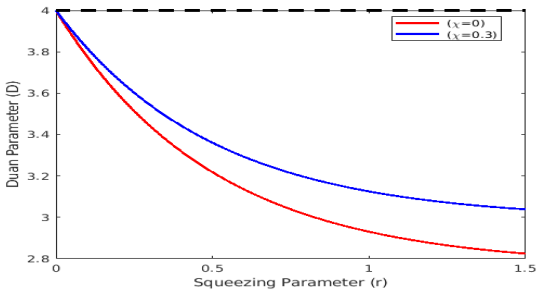


Figure 8

of Figure 8 shows how important the Kerr resonator is in improving continuous variable bipartite entanglement. As the squeezing parameter gets bigger, this improvement becomes even more noticeable, showing that the Kerr resonator helps more when the squeezing is stronger. The result shows that the Kerr nonlinear medium greatly improves continuous variable bipartite entanglement, and its effect becomes stronger as the squeezing increases because of how it works with the squeezed vacuum reservoir.

3.1 Logarithmic Negativity

Another way to examine entanglement is through logarithmic negativity, which is used for two-mode continuous variables and is based on the negativity of the partial transposition. The smallest symplectic eigenvalue of the partially transposed covariance

matrix is [24]

$$\tilde{\nu} = \sqrt{\frac{\Sigma - \sqrt{\Sigma^2 - 4\det V}}{2}}, \tag{76}$$

where,

$$\Sigma = \det A + \det B - 2\det C, \tag{77}$$

in which A and B are the covariance matrices describing each mode separately while C are the intermodal correlations.

with

$$V = \begin{pmatrix} A & C \\ C^T & B \end{pmatrix}. \tag{78}$$

The elements of the matrix on Equation are given by

$$V_{ij} = \frac{1}{2}\langle Y_i Y_j + Y_j Y_i\rangle - \langle Y_i\rangle\langle Y_j\rangle.$$

Since the fluctuations have zero mean,

$$V_{ij} = \frac{1}{2}\langle Y_i Y_j + Y_j Y_i\rangle.$$

in which i, j 1, 2, 3, 4. The quadrature operators are defined as $\hat{X}_k = (\hat{k} + \hat{k}^\dagger)/\sqrt{2}$ and $\hat{P}_k = (\hat{k} - \hat{k}^\dagger)/(i\sqrt{2})$ ($k \in \{a, b\}$ [15] where, $\mathbf{Y} = (X_a, P_a, X_b, P_b)^T$.

$$V = \begin{pmatrix} \eta & 0 & \rho & 0 \\ 0 & \eta & 0 & -\rho \\ \rho & 0 & \phi & 0 \\ 0 & -\rho & 0 & \phi \end{pmatrix}. \tag{79}$$

where the quadrature operators

$$\eta = \frac{1}{2}\left(2n_a + 1 + \alpha + \alpha^*\right), \phi = \frac{1}{2}\left(2n_b + 1 + \beta + \beta^*\right),$$
$$\rho = \frac{1}{2}\left(\gamma + \gamma^*\right) \tag{80}$$

with $n_a = \langle a^\dagger a\rangle, n_b = \langle b^\dagger b\rangle$ and $m = \langle ab\rangle$. A positive value of E_N indicates bipartite entanglement, while larger values correspond to stronger quantum correlations.

Thus, only ten independent unknowns must be determined. The logarithmic negativity for a two-mode state [38] is defined as

$$E_N = \max\left[0, -\log_2(2\tilde{\nu})\right]. \tag{81}$$

The entanglement is achieved when EN is positive with in the region of the lowest eigenvalue of covariance matrix $\nu < 1$

Figure 9 shows how the average number of photons in mode a (n_a) and mode b (n_b), along with the real part of the intermode cross-correlation function ($m = \langle ab\rangle$),

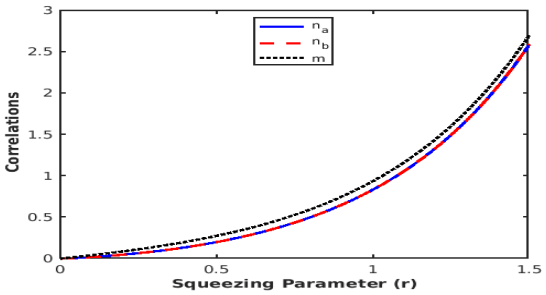


Figure 9

change as the squeezing parameter r increases.The results indicate that the average photon numbers in both cavity modes rise with more squeezing, while the intermode correlation increases and stays the main feature across the whole range of squeezing. The increase in the average number of photons comes from the combined effect of the squeezed reservoir, the cascade atomic transitions, and the Kerr nonlinear interaction. Therefore, the result shows that increasing the squeezing parameter leads to a higher photon population inside the cavity and stronger quantum correlations between the two modes, resulting in brighter and more entangled optical fields. Figure 10 shows

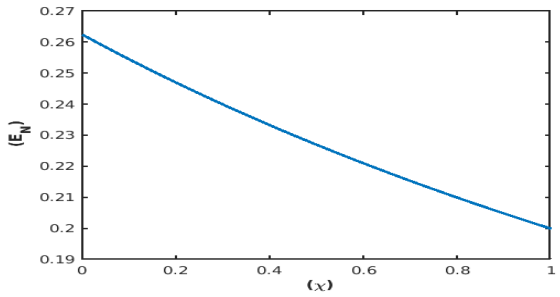


Figure 10

how the logarithmic negativity, E_N, changes as the Kerr nonlinear coefficient χ varies. As the nonlinear interaction becomes stronger, the Kerr medium causes a larger phase shift that depends on intensity, which helps the two cavity modes interact more effectively through cross-phase modulation. This leads to greater correlation between the quantum fluctuations of the two modes, improving their coherence and increasing the correlation function $\langle ab \rangle$. Thus, the Kerr nonlinear medium increases bipartite entanglement by enhancing the quantum correlations between the modes, causing a continuous rise in logarithmic negativity. Figure 11 shows how the logarithmic nega-

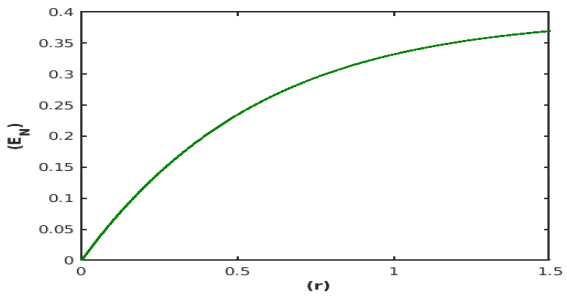


Figure 11

tivity, E_N, depends on the squeezing parameter r of the squeezed vacuum reservoir. The numerical results show that E_N increases as r increases, which means there is a gradual improvement in the entanglement between the two cavity modes.This happens because the squeezed vacuum reservoir creates strong two-photon correlations, which are described by the parameters $N = \sinh^2(r)$ and $M = \sinh(r)\cosh(r)$. As a result, the correlation between the two cavity modes becomes much stronger, leading to better quantum coherence and more entanglement, as seen by the rise in logarithmic negativity. Figure 12 shows how the logarithmic negativity, E_N, changes with the coherent

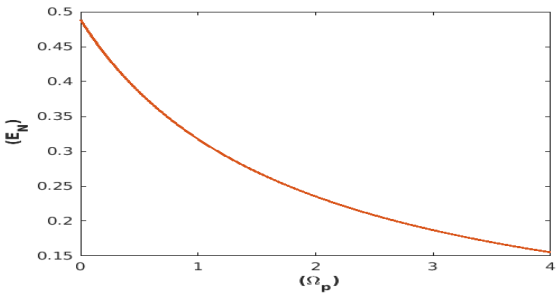


Figure 12

pump strength Ω_p.The numerical results show that as the pump strength increases, the logarithmic negativity also increases at first, which means the continuous-variable bipartite entanglement between the two cavity modes becomes stronger.This happens because a stronger pump increases the number of photons inside the cavity and improves the interaction between the three-level atoms and the cavity field. Therefore, the coherent pump field improves bipartite entanglement by boosting atom field interactions and cavity mode quantum correlations, and it reaches its highest level at the optimal pumping region. Figure 13 shows how the cavity decay rate κ affects the

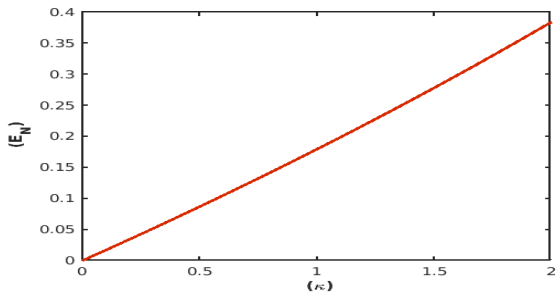


Figure 13

logarithmic negativity. When the cavity decay rate is higher, photons leave the cavity more , which lowers the number of photons inside the cavity and weakens the interaction between the three level atoms and the cavity modes. Therefore, a low cavity decay rate is important for maintaining strong continuous-variable bipartite entanglement, while higher cavity losses greatly reduce quantum correlations. Figure 14 shows

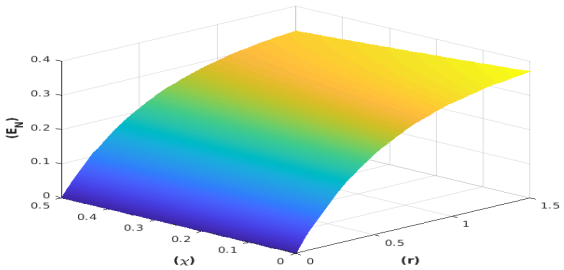


Figure 14

how the squeezing parameter r and the Kerr nonlinear coefficient χ together affect the logarithmic negativity E_N.The three-dimensional graph clearly shows that both parameters work together to improve continuous-variable bipartite entanglement in the three-level laser system. So, the squeezed vacuum reservoir and the Kerr nonlinear medium work together to create the strongest continuous variable bipartite entanglement, especially when both the squeezing parameter and the Kerr nonlinearity are large. Figure 15 compares the Duan inseparability parameter and the logarithmic negativity, E_N, as they change with the Kerr nonlinear coefficient χ. The results show that as the Kerr nonlinear coefficient increases, the Duan inseparability parameter steadily decreases and stays below the entanglement threshold ($D < 4$), which means the two cavity modes stay entangled across the whole range of parameters studied.Meanwhile,

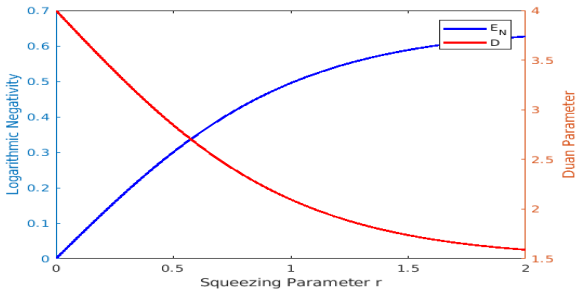


Figure 15

the logarithmic negativity keeps increasing, showing that the entanglement becomes stronger as the Kerr nonlinearity grows. So, Figure 15 shows that both the Duan inseparability criterion and logarithmic negativity support the idea that raising the Kerr nonlinear coefficient leads to more continuous-variable entanglement between the two modes.

4 Conclusion

In this work, we have theoretically investigated the generation and enhancement of bipartite entanglement in a three-level cascade laser incorporating a Kerr nonlinear resonator and coupled to a squeezed vacuum reservoir. Using the quantum master equation, we derived the Heisenbergâ Langevin equations and, under the good cavity approximation, obtained effective cavity-field equations to analyze the steadystate quantum correlations. Bipartite entanglement was quantified using both the Duan inseparability and logarithmic negativity. The results demonstrate that combining Kerr cross-phase modulation with squeezed vacuum bath driving produces a strong cooperative effect, significantly enhancing entanglement . Increasing the Kerr nonlinear coefficient and the squeezing parameter strengthens quantum correlations, while coherent pumping further improves entanglement by increasing atomic coherence and correlated photon-pair generation. Overall, the proposed system provides an efficient platform for producing bright continuous-variable entangled light with promising applications in quantum communication, teleportation, quantum networking, quantum sensing, and quantum information processing.

Author contributions Sisay Belachew, as the corresponding author, Conceptualization, Data curation, Formal Analysis, Software, Investigation, Methodology, Writing-original draft, Writing- review and editing, critically revised the manuscript for important intellectual content, and reviewed and edited the final manuscript. Firomsa Feyissa, Fantahun Talew and Mohammed Kelif conducted manuscript editing , Visualization and validated the data analysis. All authors read and approved the final manuscript.

Declarations

Ethical Statement This study is entirely theoretical and computational and does not involve human participants, human subjects, animals, or human-derived materials. Therefore, ethical approval was not required.

Consent to Participate and Consent to Publish Not applicable. This study does not involve human participants or individual-level personal data. Therefore, consent to participate and consent to publish are not applicable.

Funding The authors declare that no funds, grants, or other financial support were received during the preparation of this manuscript.

Conflict of interest The authors declare no competing interests.

Data Availability The datasets generated and analyzed during the current study are available from the corresponding author upon reasonable request.

Authors and Affiliations

Sisay Belachew*[1], Firomsa Feyissa[2], Fantahun Talew[3], Mohammed Kelif[4]

1. Department of Physics, Oda Bultum University, Chiro 226, Oromia, Ethiopia.
2. Department of Physics, Oda Bultum University, Chiro 226, Oromia, Ethiopia.
3. Department of Physics, Oda Bultum University, Chiro 226, Oromia, Ethiopia.
4. Department of Physics, Oda Bultum University, Chiro 226, Oromia, Ethiopia.

References

[1] Braunstein, S. L., and Van Loock, P. (2005). Quantum information with continuous variables. Reviews of Modern Physics, 77(2), 513–577.

[2] Duan, L. M., Giedke, G., Cirac, J. I., and Zoller, P. (2000). Inseparability criterion for continuous variable systems. Physical Review Letters, 84(12), 2722.

[3] Djordjevic, I. B. (2022). Hybrid CV-DV quantum communications and quantum networks. IEEE Access, 10, 23284–23292.

[4] Motaharifar, M., Hasani, M., & Kaatuzian, H. (2025). A survey on continuous variable quantum key distribution for secure data transmission: Toward the future of secured quantum-networks. Quantum Information & Computation, 25(2), 175–194.

[5] Sodagari, S. (2023). Integrating quantum and satellites: A new era of connectivity. IEEE Access, 11, 145101–145110.

[6] Ali, K. A. M. (2025). Physics of Squeezed and Entangled Light: A Review of Progress in Quantum Resource Generation and Applications in Quantum Communication. Scientific Journal for Publishing in Health Research and Technology, 138–146.

[7] Thakur, V. S., Kumar, A., Magarini, M., Dev, K., & Dobre, O. A. (2025). Quantum Communication and Information Technologies: A Survey on Foundation,

Error Correction, NISQ, and Networks. Authorea Preprints.

[8] Paudel, H. P., Crawford, S. E., Lee, Y. L., Shugayev, R. A., Leuenberger, M. N., Syamlal, M., ... & Duan, Y. (2023). Quantum communication networks for energy applications: Review and perspective. Advanced Quantum Technologies, 6(10), 2300096.

[9] Gessesse, M. M. (2025). The Entanglement and Quadrature Squeezing of a Cavity Light in a Coherently Pumped Atom. Bulgarian Journal of Physics, 52(3).

[10] M., Qasymeh, M., , J. (2013). Optical wave propagation in Kerr media. In *Wave Propagation Theories and Applications*. IntechOpen.

[11] Khalifa, A. S., Ahmed, H. M., Badra, N. M., & Rabie, W. B. (2024). Exploring solitons in optical twin-core couplers with Kerr law of nonlinear refractive index using the modified extended direct algebraic method. Optical & Quantum Electronics, 56(6), 1.

[12] Gashu, C., Mosisa, E., & Abebe, T. (2020). Entanglement Quantification of Correlated Photons Generated by Three-Level Laser with Parametric Amplifier and Coupled to a Two-Mode Vacuum Reservoir. Advances in Mathematical Physics, 2020(1), 9027480.

[13] Liu, S., Wang, Y., Saleem, Y., Li, X., Liu, H., Yang, C. A., ... & Liu, J. (2025). Quantum correlations of spontaneous two-photon emission from a quantum dot. Nature, 643(8074), 1234–1239.

[14] Ferretti, S., & Gerace, D. (2012). Single-photon nonlinear optics with Kerr-type nanostructured materials. Physical Review B, 85(3), 033303.

[15] Weedbrook, C., Pirandola, S., R., Cerf, N. J., Ralph, T. C., Shapiro, J. H., and Lloyd, S. (2012). Gaussian quantum information. Reviews of Modern Physics, 84(2), 621–669.

[16] Sete, E. A. (2008). Bright entangled light from two-mode cascade laser. Optics Communications, 281(24), 6124–6129.

[17] Walls, D. F., and Milburn, G. J. (2008). Quantum information. In Quantum Optics (pp. 307–346). Berlin, Heidelberg: Springer Berlin Heidelberg.

[18] Miranowicz, A., Bartkowiak, M., Wang, X., Liu, Y. X., and Nori, F. (2010). Testing nonclassicality in multimode fields: A unified derivation of classical inequalities. Physical Review A, 82(1), 013824.

[19] Knight, P. L., & Milonni, P. W. (1980). The Rabi frequency in optical spectra. Physics Reports, 66(2), 21–107.

[20] Blättermann, A., Ott, C., Kaldun, A., Ding, T., & Pfeifer, T. (2014). Two-dimensional spectral interpretation of time-dependent absorption near laser-coupled resonances. Journal of Physics B: Atomic, Molecular and Optical Physics, 47(12), 124008.

[21] Hiluf Hailu, D., & Kassahun, F. (2026). Quantum statistical properties of a three-level laser coupled to a squeezed vacuum reservoir. Journal of Optics, 28(6), 065702.

[22] Särkkä, S., & Solin, A. (2019). Applied Stochastic Differential Equations (Vol. 10). Cambridge University Press.

[23] Bowen, W. P., Lam, P. K., & Ralph, T. C. (2003). Biased EPR entanglement and its application to teleportation. Journal of Modern Optics, 50(5), 801–813.

[24] Gonzalez-Ballestero, C. (2024). Tutorial: Projector approach to master equations for open quantum systems. Quantum, 8, 1454.

[25] Abebe, T., Mosisa, E., and Gashu, C. (2021). Generation of entanglement from a two-mode cascade laser. Pramana: Journal of Physics, 95(1), 1.

[26] Vallone, M. (2026). Quantum open system description of a hybrid plasmonic cavity. Physical Review A, 113(3), 033723.

[27] Gardiner, C., and Zoller, P. (2004). Quantum Noise: A Handbook of Markovian and Non-Markovian Quantum Stochastic Methods with Applications to Quantum Optics. Springer Science and Business Media.

[28] Daley, A. J. (2005). Manipulation and simulation of cold atoms in optical lattices. na.

[29] Sirleto, L., & Righini, G. C. (2023). An introduction to nonlinear integrated photonics: Structures and devices. Micromachines, 14(3), 614.

[30] Nicholson, W. K. (2020). Linear Algebra with Applications.

[31] Mosisa, E. (2021). Enhanced Squeezing and Entanglement in Nondegenerate Three-Level Laser Coupled to Squeezed Vacuum Reservoir. Advances in Mathematical Physics, 2021(1), 6625690.

[32] Breuer, H. P., and Petruccione, F. (2002). The Theory of Open Quantum Systems. OUP Oxford.

[33] García-Beni, J., Luca Giorgi, G., Soriano, M. C., & Zambrini, R. (2024). Squeezing as a resource for time series processing in quantum reservoir computing. Optics Express, 32(4), 6733–6747.

[34] Steck, D. A. (2007). Quantum and Atom Optics.

[35] Vidal, G., and Werner, R. F. (2002). Computable measure of entanglement. Physical Review A, 65(3), 032314.

[36] Mathkoor, F. H., Kam, C. H., & Ooi, C. R. (2020). Nonclassicality of the two-photon laser with Kerr nonlinearity. Journal of the Optical Society of America B, 37(3), 820–833.

[37] Bello, L., Michael, Y., Rosenbluh, M., Cohen, E., A. (2021). Broadband complex two-mode quadratures for quantum optics. Optics Express, 29(25), 41282–41302.

[38] Boura, H. A., & Isar, A. (2015). Logarithmic negativity of two bosonic modes in the two thermal reservoir model. Romanian Journal of Physics, 60, 1278.

Figures caption

Figure 1. Schematic representation of a three-level laser via kerr resonator coupled to vacuum reservoir

Figure 2. The plot of Duan inseparability parameter is shown as a function of the squeezing parameter with the system parameters $\kappa = 1.0$, $\mu_a = \mu_b = 1.5$, $\nu_a = \nu_b = 0.6$, and $\phi^2 = 0$. When $D < 4$ [8], the two mode state meets the Duan criterion for quantum inseparability, indicating entanglement is present

Figure 3. The Duan inseparability parameter $D = \Delta u^2 + \Delta v^2$ depends on the Kerr nonlinear coefficient χ in a two-mode nonlinear system with the parameters $\kappa = 1.0$, $g_a = g_b = 2.0$, $\gamma = 5.0$, squeezing parameter $r = 1.5$, and pump strength $\Omega_p = 1.5$. The change in D as χ varies shows how Kerr nonlinearity affects the quantum correlations between the two modes.

Figure 4. The Duan inseparability parameter $D = \Delta u^2 + \Delta v^2$ is plotted against the pump strength Ω_p for a two-mode nonlinear quantum system with parameters $\kappa = 1.0$, $g_a = g_b = 2.0$, $\gamma = 5.0$, squeezing parameter $r = 0.5$, and Kerr nonlinear coefficient $\chi = 0.5$. When $D < 4$, the system is entangled according to the Duan criterion, and the variation of D with Ω_p highlights how the pump strength influences the creation and control of quantum correlations between the two modes.

Figure 5 The average number of photons inside the cavity, depends on the squeezing parameter in a two-mode nonlinear quantum system with the parameters $\kappa = 1.0$, $g_a = g_b = 2.0$, $\gamma = 5.0$, Kerr nonlinear coefficient $\chi = 0.3$, and pump strength $\Omega_p = 1.5$. As the squeezing parameter r increases, the average photon number inside the cavity also increases, which indicates a stronger effect of quantum fluctuations and influenced by the nonlinear coupling parameters.

Figure 6. The real part of the intermode correlation, $\mathrm{Re}\langle ab\rangle$, is shown as it changes with the squeezing parameter r in a two-mode nonlinear quantum system with of uses the parameters $\kappa = 1.0$, $g_a = g_b = 2.0$, $\gamma = 5.0$, Kerr nonlinear coefficient $\chi = 0.3$, and pump strength $\Omega_p = 1.5$. As the squeezing parameter increases, the correlation also increases, showing that the two-mode quantum coherence becomes stronger due to the nonlinear interaction and the squeezed input field.

Figure 7. The three-dimensional representation shows how the Duan inseparability parameter $D = \Delta u^2 + \Delta v^2$ changes with the squeezing parameter r and the Kerr nonlinear coefficient χ in a two-mode nonlinear quantum system using the values $\kappa = 1.0$, $g_a = g_b = 2.0$, $\gamma = 5.0$, and pump strength $\Omega_p = 1.5$. This indicates how squeezing and nonlinear interaction strength influence the creation of continuous-variable quantum correlations.

Figure 8. The Duan inseparability parameter $D = \Delta u^2 + \Delta v^2$ is compared as a function of the squeezing parameter r, both with and without Kerr nonlinear interaction with parameters $\kappa = 1.0$, $g_a = g_b = 2.0$, $\gamma = 5.0$, pump strength $\Omega_p = 1.5$. This comparison highlights how Kerr nonlinearity affects the creation and changes in two-mode quantum correlations as the squeezing strength increases.

Figure 9. The mean photon numbers n_a, n_b, and the intermode correlation term $m = \mathrm{Re}\langle ab\rangle$ are shown as they change with the squeezing parameter r in a two-mode quantum system with using the parameters $\kappa = 1.0$, $\mu_a = \mu_b = 1.5$, $\nu_a = \nu_b = 0.6$, and a squeezing phase $\phi_{\mathrm{sq}} = 0$. As the squeezing parameter increases, both the photon

numbers and the intermode correlations rise, indicating that the squeezed input field boosts quantum fluctuations and the correlations between the two modes.

Figure 10. The graph shows how the logarithmic negativity E_N changes with the Kerr nonlinear coefficient χ in a two-mode quantum system with the parameters $\kappa = 1.0$, squeezing parameter $r = 0.6$, squeezing phase $\phi_{\text{sq}} = 0$, $\mu_{\text{base}} = 1.5$, and $\nu_{\text{base}} = 0.6$. As χ increases, E_N also increases, showing that the quantum entanglement between the two modes improves due to the Kerr nonlinear interaction.

Figure 11. The graph shows how the logarithmic negativity E_N changes with the squeezing parameter r in a two-mode quantum system with parameters $\kappa = 1.0$, $\mu_a = \mu_b = 1.5$, $\nu_a = \nu_b = 0.6$, and a squeezing phase $\phi_{\text{sq}} = 0$. As the squeezing parameter increases, E_N also increases, showing that stronger two-mode squeezing leads to more quantum entanglement.

Figure 12. The dependence of logarithmic negativity E_N on the pump strength Ω_p is shown for a two-mode quantum system uses fixed values of $\kappa = 1.0$, squeezing parameter $r = 0.5$, and squeezing phase $\phi_{\text{sq}} = 0$. As the pump strength increases, the variation in E_N shows how the external driving field affects the creation and strengthening of steady state quantum entanglement between the two modes.

Figure 13. The logarithmic negativity E_N depends on the coupling/dissipation parameter κ in a two-mode quantum system with use the parameters $r = 0.5$, squeezing phase $\phi_{\text{sq}} = 0$, $\mu_{\text{base}} = 1.5$, $\nu_{\text{base}} = 0.6$, and Kerr nonlinear coefficient $\chi = 1$.The effective parameters are adjusted to $\mu_a = \mu_b = \mu_{\text{base}} + 0.1\chi$ and $\nu_a = \nu_b = \nu_{\text{base}} + 0.5\chi$. As the result, the quantum entanglement between the two modes, showing how the parameter κ affects the strength of steady-state quantum correlations.

Figure 14. The three-dimensional plot shows how the logarithmic negativity E_N depends on the squeezing parameter r and the Kerr nonlinear coefficient χ in a two-mode quantum system using the parameters $\kappa = 1.0$, $\mu_{\text{base}} = 1.5$, $\nu_{\text{base}} = 0.6$, and squeezing phase $\phi_{\text{sq}} = 0$. The surface demonstrates how both squeezing and Kerr nonlinearity affect the creation of entanglement, highlighting that stronger nonlinear interactions and higher squeezing can lead to greater quantum correlations in the steady state.

Figure 15. The graph shows how the logarithmic negativity E_N and the Duan inseparability parameter D change with the squeezing parameter r.